Journal of Chromatography A, 1217 (2010) 2132–2137

Contents lists available at ScienceDirect

Journal of Chromatography A

journal homepage: www.elsevier.com/locate/chroma

A thermodynamically consistent explicit competitive adsorption isotherm model based on second-order single component behaviour

Milica Ilić[a,1], Dietrich Flockerzi[a], Andreas Seidel-Morgenstern[a,b,*]

[a] Max Planck Institute for Dynamics of Complex Technical Systems, Sandtorstrasse 1, D-39106 Magdeburg, Germany
[b] Otto von Guericke University, Chair of Chemical Process Engineering, Universitätsplatz 2, D-39106 Magdeburg, Germany

ARTICLE INFO

Article history:
Received 29 November 2009
Received in revised form 28 January 2010
Accepted 2 February 2010
Available online 10 February 2010

Keywords:
Adsorption isotherms
Binary mixture
Ideal adsorbed solution theory
Langmuir isotherm
Quadratic isotherm

ABSTRACT

A competitive adsorption isotherm model is derived for binary mixtures of components characterized by single component isotherms which are second-order truncations of higher order equilibrium models suggested by multi-layer theory and statistical thermodynamics. The competitive isotherms are determined using the ideal adsorbed solution (IAS) theory which, in case of complex single component isotherms, does not generate explicit expressions to calculated equilibrium loadings and causes time consuming iterations in simulations of adsorption processes. The explicit model derived in this work is based on an analysis of the roots of a cubic polynomial resulting from the set of IAS equations. The suggested thermodynamically consistent and widely applicable competitive isotherm model can be recommended as a flexible tool for efficient simulations of fixed-bed adsorber dynamics.

1. Introduction

The competitive adsorption isotherms are the most essential information which should be provided to design and optimize separation processes based on selective adsorption [1,2]. Still the most reliable way to obtain isotherms is to perform experiments [3]. Unfortunately, the experimental determination of competitive isotherms is difficult and time consuming. Therefore, competitive isotherms are typically predicted using thermodynamic models exploiting knowledge about the single component isotherms, which can be easier measured. One of the most successful and widely applied models is the ideal adsorbed solution (IAS) theory [4]. Although real systems can deviate from ideality [5], the thermodynamically consistent competitive isotherms predicted by the IAS theory are very useful in simulating, designing and optimizing adsorption processes.

Explicit forms of competitive isotherm models based on the IAS theory are available only for a few relatively simple single component isotherm models (e.g. the Henry and Langmuir equations [4]). For more complex single component models explicit solutions of the IAS theory are not available and, therefore, the competitive isotherms have to be calculated numerically using iterative procedures.

In order to extend the library of the available thermodynamically consistent competitive isotherm models, the main task of this theoretical study is to find an explicit solution for the case of second-order truncations of single component isotherms ("quadratic isotherms"), which are suggested by various theoretical concepts and which are more flexible and, thus, often more accurate. These second-order models are e.g. capable to describe frequently observed inflection points in the isotherm courses.

In order to validate the derived explicit competitive isotherm model, predicted equilibrium loadings will be compared with results of corresponding numerical solutions. Additionally, the obtained isotherm model will be used in numerical simulations of fixed-bed dynamics, again in comparison with simulations based on solving iteratively the set of IAS equations.

2. Single component adsorption isotherms

The most often used nonlinear single component adsorption isotherm model is the Langmuir model [1,3,6] which correlates the fluid phase concentrations C_i^0 of a component i and the corresponding equilibrium loading of the solid phase, Q_i^0, as follows:

$$Q_i{}^0(C_i{}^0) = Q_{sat,i}\frac{b_i C_i{}^0}{1 + b_i C_i{}^0} \quad (1)$$

* Corresponding author at: Otto von Guericke University, Chair of Chemical Process Engineering, Universitätsplatz 2, D-39106 Magdeburg, Germany.
Tel.: +49 3916718644; fax: +49 3916712028.
E-mail address: seidel-morgenstern@mpi-magdeburg.mpg.de
(A. Seidel-Morgenstern).
[1] Present address: Daimler AG, D-73230 Kirchheim unter Teck/Nabern, Germany.

0021-9673/$ – see front matter © 2010 Elsevier B.V. All rights reserved.
doi:10.1016/j.chroma.2010.02.006

Nomenclature

A	defined in Eq. (13a) [g/l]
$b_{i,1}$	parameter of the adsorption isotherm model, Eq. (4) [l/g]
$b_{i,2}$	parameter of the adsorption isotherm model, Eq. (4) [l^2/g^2]
B	defined in Eq. (13b) [g/l]
C	defined in Eq. (13c) [g/l]
C_i	concentration of component i in the liquid phase [g/l]
C^0	single solute concentration [g/l]
$C^{0,fic}$	hypothetical single solute concentration [g/l]
C^{inj}	injection concentration [g/l]
C^{mix}	liquid phase concentration in mixture [g/l]
D	defined in Eq. (13d) [g/l]
D_{app}	apparent axial dispersion coefficient [m^2/s]
f_*	defined in Eq. (15) [g/l]
F	cubic polynomial, defined in Eq. (12) [g/l]
l	column length [m]
N	number of components present in a mixture
N_p	number of theoretical plates, Eq. (18)
Q	concentration in the solid phase [g/l]
$Q_{sat,i}$	saturation capacity (parameter of the adsorption isotherm model) [g/l]
Q_{tot}	total loading [g/l]
Q^{mix}	loading in mixture [g/l]
R	universal gas constant [J/g K]
S_{ads}	adsorbent surface [m^2]
t	time coordinate [s]
T	temperature [K]
u	linear velocity [m/s]
V_{ads}	adsorbent volume [m^3]
V^{inj}	injection volume [l]
x	space coordinate [m]
z	molar fraction
z_*	defined in Eq. (15)

Greek symbols

α	defined in Eq. (14)
β	defined in Eq. (14), [l/g]
γ	defined in Eq. (14), [l/g]
δ	defined in Eq. (15)
ξ	running variable in Eq. (8), corresponding to single solute concentration [g/l]
ε	total porosity
λ_0	RTV_{ads}/S_{ads}, Eq. (8) [J m/g]
θ_*	defined in Eq. (15)
ν	defined in Eq. (2)
π	spreading pressure, Eq. (8) [J/m^2]

In this equation $Q_{sat,i}$ is the saturation (maximum) capacity of the solid phase and b_i is a positive temperature dependent parameter quantifying the adsorption energy. This classical model assumes that each adsorption site is energetically equivalent and is available only for one molecule. Molecular interactions between the molecules adsorbed are neglected. Eq. (1) accounts only for loadings up to the formation of so-called mono-layers.

Experimentally observed isotherms are often characterized by more complex isotherm shapes, which can not be described accurately by Eq. (1) [7]. A typical feature is the occurrence of inflection points in the isotherm courses, which can be caused, e.g. by multi-layer formation, the presence of energetically heterogeneous adsorbent surfaces, lateral interactions between adsorbed molecules and capillary condensation phenomena. In order to describe more complex isotherms shapes, various models have been suggested. A very general and flexible model was suggested by Hill [8]. It results from classical concepts of statistical thermodynamics applied to adsorption equilibria. The model can be expressed in the following special form of a Mth order Padé approximant [9]:

$$Q_i^0(C_i^0) = Q_{sat,i}^* C_i^0 \frac{\left[d\nu_i(C_i^0)/dC_i^0\right]}{\nu_i(C_i^0)} \quad \text{with}$$

$$\nu_i(C_i^0) = 1 + \sum_j^M b_{i,j}(C_i^0)^j \tag{2}$$

The $b_{i,j}$ are positive parameters quantifying varies types of interaction energies. For $M=1$ Eq. (2) reduces to Eq. (1). For the second-order approximation ($M=2$) holds:

$$\nu_i(C_i^0) = 1 + b_{i,1}C_i^0 + b_{i,2}C_i^{02} \tag{3}$$

This leads to the following well known quadratic isotherm model [1,10,11].

$$Q_i^O(C_i^0) = \frac{Q_{sat,i}^* C_i^0 (b_{i1} + 2b_{i2}C_i^0)}{1 + b_{i1}C_i^0 + b_{i2}C_i^{02}} \tag{4}$$

Eq. (4) is quite flexible and capable of describing inflection points in the isotherm courses. The same quadratic isotherm model given by Eq. (4) can be also derived exploiting the extended BET-theory [11] or using a lattice model [12]. If the liquid phase concentration approaches infinity, Eq. (4) predicts that the solid phase concentration reaches a saturation value $Q_{sat,i} = 2Q_{sat,i}^*$.

3. Derivation of competitive adsorption isotherm model for a binary system

A well-known and widely used extension of the Langmuir model (Eq. (1)) to the case of competitive adsorption of N components in a mixture is [1,2]:

$$Q_i^{mix}(C_1^{mix}, \ldots, C_N^{mix}) = Q_{sat,i} \frac{b_i C_i^{mix}}{1 + \sum_{k=1}^N b_k C_k^{mix}} \quad i = 1, N \tag{5}$$

This equation predicts the loadings of a component i in the mixture, Q_i^{mix}, as a function of the fluid phase concentrations C_k^{mix}. It is thermodynamically consistent only if the saturation capacities are the same for all components [13], i.e.:

$$\bar{Q}_{sat} = Q_{sat,i} \quad i = 1, N \tag{6}$$

The most successful and often applied approach to derive competitive isotherms from single component data is the ideal adsorbed solution (IAS) theory. This theory was initially developed by Myers and Prausnitz [4] for gas adsorption and extended to treat adsorption from dilute liquid solutions by Radke and Prausnitz [14]. An important advantage of the IAS theory is that it provides for any set of single component isotherms thermodynamically consistent competitive isotherms.

Using the framework of IAS theory, for a N component mixture, characterized by the N independent fluid phase concentrations $C_1^{mix}, \ldots, C_N^{mix}$, the following $2N+1$ equations have to be solved simultaneously to determine the $2N+1$ dependent variables $C_1^{0,fic}, \ldots, C_N^{0,fic}, Q_1^{mix}, \ldots, Q_N^{mix}, Q_{tot}^{mix}$ [4,14]:

$$\pi_i(C_i^{0,fic}) = \pi_{i+1}(C_{i+1}^{0,fic}) \quad i = 1, N-1 \tag{7a}$$

$$\sum_{k=1}^{N} \frac{C_k^{mix}}{C_k^{0,fic}} = 1 \tag{7b}$$

$$\sum_{k=1}^{N} \frac{Q_k^{mix}}{Q_k^0(C_k^{0,fic})} = 1 \tag{7c}$$

$$\frac{Q_i^{mix}}{Q_{tot}^{mix}} = \frac{C_i^{mix}}{C_i^{0,fic}} \quad i = 1, N \tag{7d}$$

Because of Eq. (7d), Eq. (7c) can be replaced by:

$$\frac{1}{Q_{tot}^{mix}} = \sum_{k=1}^{N} \frac{C_k^{mix}}{C_k^{0,fic} Q_k^0(C_k^{0,fic})} \tag{7e}$$

An important tool of the theory is the Gibbs adsorption isotherm which quantifies the two-dimensional spreading pressure (π) present in the adsorbed phase (Eq. (7a)). The $C_i^{0,fic}$ are hypothetical (fictive) concentrations of a component i in a hypothetical single component system, which generate the same spreading pressure as the mixture does. The Q_i^{mix} are the equilibrium loadings of component i to be determined and Q_{tot}^{mix} is the total equilibrium loading.

The spreading pressures of a single component i for the fictive concentration $C_i^{0,fic}$ can be determined from the single component Gibbs adsorption equation as [4,14]:

$$\pi_i(C_i^{0,fic}) = \lambda_0 \int_0^{C_i^{0,fic}} \frac{Q_i^0(\xi)}{\xi} d\xi \quad i = 1, N \tag{8}$$

Hereby λ_0 substitutes RTV_{ads}/S_{ads} and Q_i^0 stands for the single component isotherm model.

Provided Eq. (6) holds, the set of Eqs. (7) and (8) can be solved analytically for the Langmuir single component isotherms (Eq. (1)). The result is the expression given by Eq. (5). Solving Eqs. (7) and (8) is more complex for almost all other single component isotherm models. If Eq. (6) does not hold, already in case of applying Eq. (1) numerical methods must be used.

Below we present an explicit competitive isotherm model for the two components of a binary mixture using the IAS theory and Eq. (4) for the single solute isotherms. In addition it is assumed that Eq. (6) holds. In this case the spreading pressure expression, Eq. (8), provides:

$$\pi_i(C_i^{0,fic}) = \lambda_0 \tilde{Q}_{sat} \ln[1 + b_{i,1} C_i^{0,fic} + b_{i,2} (C_i^{0,fic})^2] \quad i = 1, 2 \tag{9}$$

Using Eqs. (7a) and (9) leads to:

$$1 + b_{1,1} \frac{C_1^{mix}}{z_1} + b_{1,2} \left[\frac{C_1^{mix}}{z_1}\right]^2 = 1 + b_{2,1} \frac{C_2^{mix}}{z_2} + b_{2,2} \left[\frac{C_2^{mix}}{z_2}\right]^2 \tag{10}$$

Hereby, following a suggestion made recently [15], adsorbed phase molar fractions z_i have been introduced for the hypothetical concentrations $C_i^{0,fic}$ (see Eq. (7d)):

$$z_i = \frac{C_i^{mix}}{C_i^{0,fic}} \quad i = 1, 2 \quad \text{with} \quad z_2 = 1 - z_1 \tag{11}$$

Eq. (10) can be reformulated as $F = 0$ for the following cubic polynomial F with $(x, y) \equiv ({C_1}^{mix}, {C_2}^{mix}) \in \Re_+^2$ and $z \equiv z_1$:

$$F(x, y, z) = A(x, y) z^3 + B(x, y) z^2 + C(x, y) z + D(x, y) \tag{12}$$

with

$$A(x, y) = \alpha x + y > 0 \tag{13a}$$

$$B(x, y) = x(\beta x - 2\alpha) - y(1 + \gamma y) \tag{13b}$$

$$C(x, y) = x(\alpha - 2\beta x) \tag{13c}$$

$$D(x, y) = \beta x^2 \geq 0 \tag{13d}$$

and the parameters

$$\alpha = \frac{b_{1,1}}{b_{2,1}} > 0, \quad \beta = \frac{b_{1,2}}{b_{2,1}} \geq 0, \quad \gamma = \frac{b_{2,2}}{b_{2,1}} \geq 0$$

$$\text{for} \quad b_{i,1} > 0, \quad b_{i,2} \geq 0 \quad i = 1, 2 \tag{14}$$

The zero of F in [0,1] solving Eq. (10) provides the z_1 we are looking for. In Appendix A, following [16], is given the derivation of this unique zero in [0,1] designated as z^{II}. The derived analytical expression is:

$$z_1 = z^{II} \equiv z^{II}(x, y) = z^{II}(C_1^{mix}, C_2^{mix})$$
$$= z_*(x, y) + 2\delta(x, y) \cos\left(\theta_*(x, y) + \frac{4\pi}{3}\right) \in [0, 1] \tag{15, A5b}$$

with

$$z_*(x, y) = \frac{-B(x, y)}{[3A(x, y)]}$$

$$\delta \equiv \delta(x, y) = \frac{[B^2(x, y) - 3A(x, y)C(x, y)]^{1/2}}{[3A(x, y)]}$$

$$\theta_* \equiv \theta_*(x, y) = \frac{1}{3} \arccos\left(-\frac{f_*(x, y)}{2A(x, y)\delta^3(x, y)}\right) \in \left[0, \frac{\pi}{3}\right]$$

$$f_*(x, y) = F(x, y, z_*(x, y))$$

Using this expression for $z_1(C_1^{mix}, C_2^{mix}) = z^{II}$ and Eq. (7e), the equilibrium loadings Q_i^{mix} can be determined as follows:

$$Q_i^{mix}({C_1}^{mix}, {C_2}^{mix}) = Q_{tot}^{mix} z_i = \left[\frac{z_1}{Q_1^0(C_1^{0,fic})} + \frac{1 - z_1}{Q_2^0(C_2^{0,fic})}\right]^{-1} z_i$$

$$i = 1, 2 \tag{16a}$$

with

$$C_1^{0,fic} = \frac{{C_1}^{mix}}{z_1}, \quad C_2^{0,fic} = \frac{{C_2}^{mix}}{(1 - z_1)} \tag{16b}$$

This solution allows direct calculation of competitive IAS isotherms involving two second-order single component isotherm models $Q_1^0({C_1}^0)$ and $Q_2^0({C_2}^0)$. It is also valid for binary mixtures involving a combination of first and second-order truncations (Langmuir and quadratic isotherms) and can be efficiently applied in simulations of fixed-bed dynamics, where typically a large amount of equilibrium calculations has to be performed.

4. Application of the derived competitive isotherm model

4.1. Equilibrium loadings

For illustration and also to check the derived analytical competitive adsorption isotherm equation, the following parameters were used in the single solute isotherm model (Eq. (4)): $Q_{sat,1}^* = Q_{sat,2}^* = 5$ g/l, $b_{1,1} = 1$ l/g, $b_{1,2} = 2\,\mathrm{l}^2/\mathrm{g}^2$, $b_{2,1} = 2$ l/g, $b_{2,2} = 3\,\mathrm{l}^2/\mathrm{g}^2$. In addition to applying Eqs. (13)–(16), numerical solutions of Eqs. (7) and (8) were calculated using three methods implemented in Matlab [17], i.e. the Gauss–Newton, the Levenberg–Marquardt and Trust-Region-Dogleg methods. A general survey regarding these well established nonlinear least-square methods is given in [18]. Details concerning the Levenberg–Marquardt method can be found in [19,20], while

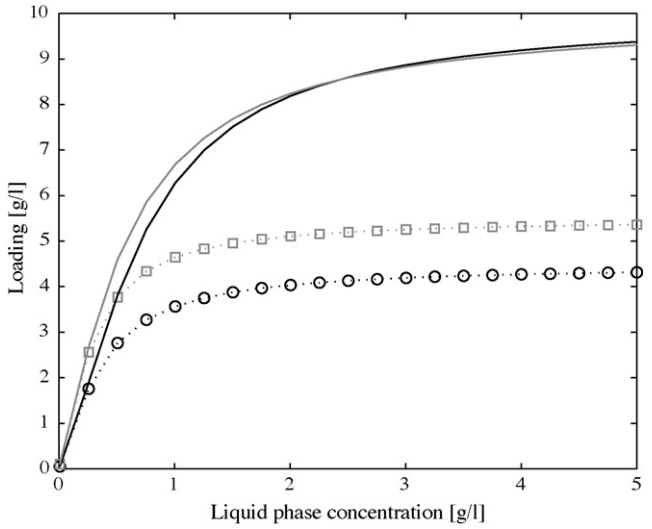

Fig. 1. Comparison of the derived analytical solution (Eqs. (13)–(16)) and results of numerical calculations solving Eqs. (7) and (8). The single component isotherms (solid lines) correspond to Eq. (4) and the parameters given in the text. Black-component 1, grey-component 2, squares and circles—derived analytical solution, dotted lines—numerical solutions (1:1 mixtures).

an overview regarding the Trust-Region-Dogleg method is given in [21].

In Fig. 1 are presented the single solute isotherms of the two components as solid lines. The existence of the inflection points in the courses of these two isotherms is hardly visible in this presentation. To illustrate this feature better plots of the isotherm derivatives dQ/dC vs. C or of Q/C vs. C are more suitable. For the sake of brevity they are not given here. Selected competitive isotherms are given in Fig. 1 for 1:1 mixtures in the liquid phase, i.e. $C_1^{mix} = C_2^{mix}$. The expected reduction of loadings in the mixture case can be clearly seen. Of importance for the purpose of this study is the fact that the squares and circles, corresponding to the analytical solution, coincide perfectly with the numerical results shown as dotted lines. Regarding the latter there were no significant differences found for the three methods applied. However, the Gauss–Newton method was not able to provide for some pairs of C_1^{mix} and C_2^{mix} the solution with the default parameters of the solver.

The derived analytical solution can be also reduced to describe the case, where one of the isotherms is only of the first-order type. The combination of first-order (Langmuir) and second-order (quadratic, BET) types of single component isotherms was analysed in detail in [22]. Results of using Eqs. (13)–(16) were compared again with corresponding numerical solutions for such a situation. The single component isotherm parameters used are related to the adsorption of Tröger's base enantiomers on microcrystalline cellulose triacetate with ethanol as solvent. In [23] this system was studied theoretically and experimentally. It was found that the isotherm of the (−)-enantiomer, which elutes first, is of the Langmuir type (Eq. (1)), while the isotherm of the (+)-enantiomer has an inflection point and can be modelled with the quadratic isotherm model (Eq. (4)). The single solute isotherm model parameters used here were taken from the parameters fitted in [23] to experimental data (just the saturation capacities were slightly modified to guarantee consistency): $Q_{sat,1} = \bar{Q}_{sat} = 20\,g/l$, $b_{1,1} = 0.157\,l/g$, $b_{1,2} = 0\,l^2/g^2$, $Q^*_{sat,2} = \bar{Q}_{sat}/2 = 10\,g/l$, $b_{2,1} = 0.948\,l/g$, $b_{2,2} = 1.072\,l^2/g^2$. The obtained isotherms are presented in Fig. 2. There is a strong reduction in the equilibrium loadings of the (−)-enantiomers in 1:1 mixtures, which is due to the relatively large separation factor and also the pronounced inflection point in the course of the single component isotherm of the (+)-enantiomer. As in the first example no differences were found between the competitive isotherms calculated analytically and numerically. The presence of inflection points is known to be the reason for unusual peak shapes if efficient chromatographic columns are applied [24]. To investigate this phenomenon the isotherms of this second example were applied within a model capable to predict column dynamics.

4.2. Application of the derived competitive isotherm model in fixed-beds models

The equilibrium-dispersive model [1] as one of the most frequently applied model was used to predict the development of concentration profiles in fixed-beds. This model assumes isothermal conditions and that the liquid and solid phases are permanently and at all local positions in equilibrium. Radial gradients are neglected and it is further assumed that all band broadening contributions (due to, e.g. axial dispersion and finite rates of mass transfer processes) can be lumped into an apparent axial dispersion coefficient. The corresponding mass balance for a component i in a N component mixture is [1]:

$$\frac{\partial C_i^{mix}}{\partial t} + \frac{1-\varepsilon}{\varepsilon} \cdot \frac{\partial Q_i^{mix}(C_1^{mix}, \ldots, C_N^{mix})}{\partial t} + u\frac{\partial C_i^{mix}}{\partial x} = D_{app,i}\frac{\partial^2 C_i^{mix}}{\partial x^2},\ i = 1, 2, \ldots, N \quad (17)$$

where the C^{mix} are again the concentrations in the fluid phase, the Q^{mix} the corresponding equilibrium concentrations in the solid phase, t the time coordinate and x is the space coordinate. Further, ε is the total column porosity, u the interstitial fluid phase velocity and D_{app} the apparent axial dispersion coefficient. For efficient columns (small $D_{app,i}$ values) and similar dispersion behaviour of all components ($\bar{D}_{app} = D_{app,i}$) can be assumed [1]:

$$N_p = \frac{ul}{2\bar{D}_{app}} \quad (18)$$

In this equation N_p stand for the number of theoretical plates, which is typically applied to evaluate the efficiency of chromatographic columns, and l for the column length.

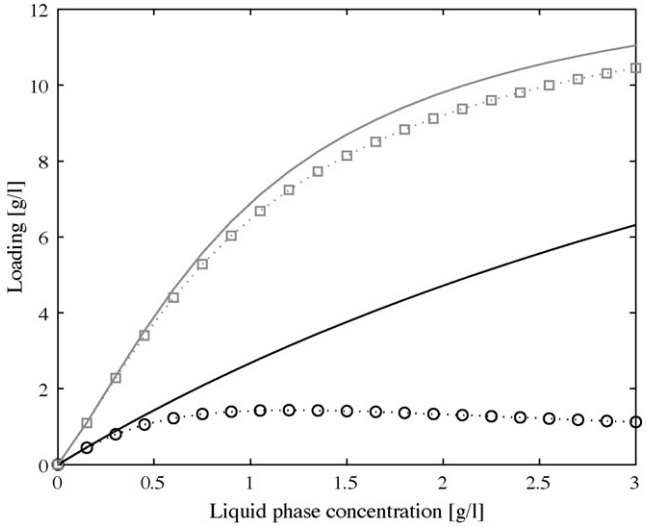

Fig. 2. Comparison of the derived analytical solution (Eqs. (13)–(16)) and results of numerical calculations solving Eqs. (7) and (8). Single component isotherms (solid lines) follow Eq. (1) (component 1, (−)-enantiomer, black) and Eq. (4) (component 2, (+)-enantiomer, grey), respectively, for the parameters given in the text. Squares and circles—derived analytical solution, dotted lines—numerical solutions (1:1 mixtures).

Suitable boundary conditions valid for fixed-bed adsorption have been suggested by Dankwerts [25]. Analytical solutions of Eq. (17) can be derived only for linear adsorption isotherms. Otherwise numerical methods must be applied. In this study a finite difference method with forward-in-space and backward-in-time approximations [26] was used, combined with both the analytical solution for the local equilibrium (Eqs. (13)–(16)) and the numerical solution of Eqs. (7) and (8) The technique is based on solving efficiently a reduced form of Eq. (16) (setting the right-hand side to zero) on a coarse grid. The following expression for the liquid phase concentration of a component i at the space position $n+1$ and the time position j represents the scheme:

$$C^j_{i,n+1} = C^j_{i,n} - \frac{\Delta x}{u\Delta t}\left[C^j_{i,n} - C^{j-1}_{i,n} + \frac{1-\varepsilon}{\varepsilon}\left(Q^j_{i,n} - Q^{j-1}_{i,n}\right)\right] \quad i = 1, N \tag{19}$$

The Δx and Δt are the space and time increments, respectively, chosen in a way that numerical and physical dispersions match [26]. The Courant–Friedrichs–Lewy convergence condition provides a limit for the Courant number a_{cou} in order to assure stability of the scheme [27]:

$$a_{cou} = u\frac{\Delta t}{\Delta x} \geq 1 \tag{20}$$

Although the described numerical method (as also other alternatives) is relatively fast using modern computers, there is still a significant amount of computation time needed if the equilibrium loadings of the compounds involved are not given via explicit expressions. To demonstrate the potential of the derived analytical solutions of the IAS theory, elution profiles were calculated for the isotherms identified for the Tröger's base enantiomers dissolved in ethanol in contact with microcrystalline cellulose triacetate. As in [23] the following parameters were used: a column length of $l = 25$ cm, an internal column diameter of 4.6 mm, a total column porosity of $\varepsilon = 0.66$, number of theoretical plates $N_P = 138$, volumetric flow-rate of 0.5 ml/min, injection concentrations $C_1^{inj} = C_2^{inj} = 1.5$ g/l. In four calculations the injection volume was increased stepwise ($V^{inj} = 6$, 8, 10 and 12 ml).

Fig. 3a–d illustrate elution profiles for both enantiomers calculated with $a_{cou} = 2.3$ as well as the corresponding total concentration profiles. Only very small (in the figures hardly to detect) discrepancies were found between the profiles generated using the analytical and numerical solutions of the IAS isotherm model. However, the times required for these simulations differed significantly. On an ordinary PC the calculation of an elution profile using Eqs. (13)–(16) took less than 2 s, while the numerical calculation required significantly more time (several minutes up to hours, depending on the method used and the starting values provided).

The elution profiles shown in Fig. 3 for this series of volume overloading reveal the strong impact of the inflection point in the isotherm of the longer retained second component (the (+)-enantiomer of Tröger's base) on the band shapes. The courses of the desorption branches of the second component clearly reveal the dispersed (Langmuirian) behaviour for concentrations above the isotherm inflection point followed by a shock for lower concentrations (anti-Langmuirian behaviour). The competition between the two components leads to effluent concentrations of the first eluting component (the (−)-enantiomer) clearly above the injection concentration.

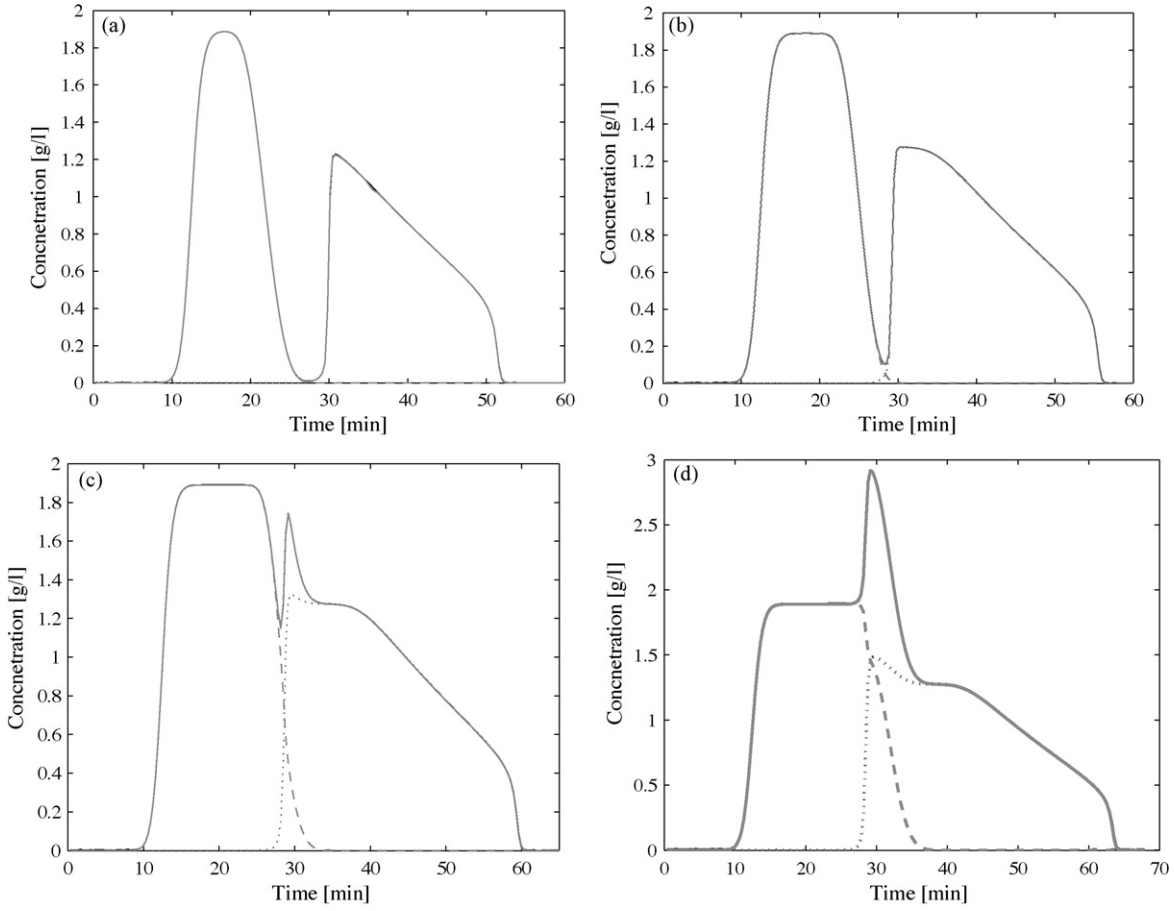

Fig. 3. Elution profiles predicted with the equilibrium-dispersive model using the isotherm parameters underlying Fig. 2 and the additional parameters given in the text. Varied parameter was the injection volume: (a) 6 ml, (b) 8 ml, (c) 10 ml and (d) 12 ml. Solid line—total concentration; dashed and dotted lines (partly hidden)—components 1 and 2. Hardly to distinguish: black line—numerical solution of equilibrium model, grey line—analytical equilibrium model (Eqs. (13)–(16)).

It should be finally mentioned that the course of predicted elution profiles will be of course also influenced by the fixed-bed model used and the kinetic parameters included. For models more detailed then the equilibrium-dispersive model, the application of explicit isotherm expressions can be computationally even more beneficial than for the case presented here for illustration.

5. Conclusions

An explicit adsorption isotherm model was derived for binary mixtures using the IAS theory. The model is applicable for components characterized by second-order single component isotherms. Eqs. (13)–(16) allow for rapid and thermodynamically consistent calculation of the concentrations in the solid phase without requiring numerical methods. The solution derived can be implemented easily in any fixed-bed model reducing there significantly the computation time. Due to its flexibility it can be very helpful in designing and optimizing various types of adsorption processes.

Acknowledgements

The support of Deutsche Forschungsgemeinschaft (SFB 578) and Fonds der Chemsichen Industrie is gratefully acknowledged.

Appendix A.

Here will be given more details on the derivation of the obtained general isotherm model following [16]. We show that the polynomial $F(x,y,z)$ (Eq. (12)) possesses for $(x,y)\in\Re_+^2$ three real simple zeros

$$z^{\mathrm{I}}(x,y)\le 0 < z^{\mathrm{II}}(x,y) < 1 \le z^{\mathrm{III}}(x,y) \tag{A1}$$

If we define the point of symmetry of the cubic F as:

$$(z_*(x,y), f_*(x,y)) \quad \text{with} \quad z_*(x,y) = \frac{-B(x,y)}{[3A(x,y)]},$$

$$f_*(x,y) = F(x,y,z_*(x,y)) \tag{A2}$$

and introduce the positive

$$\delta \equiv \delta(x,y) := \frac{[B^2(x,y) - 3A(x,y)C(x,y)]^{1/2}}{[3A(x,y)]} \tag{A3}$$

and the angle

$$\theta_* \equiv \theta_*(x,y) := \frac{1}{3}\arccos\left(-\frac{f_*(x,y)}{2A(x,y)\delta^3(x,y)}\right) \in \left[0, \frac{\pi}{3}\right] \tag{A4}$$

then the zeros of F are given by

$$z^{\mathrm{I}} \equiv z^{\mathrm{I}}(x,y) = z_*(x,y) + 2\delta(x,y)\cos\left(\theta_*(x,y) + \frac{2\pi}{3}\right) \le 0, \tag{A5a}$$

$$z^{\mathrm{II}} \equiv z^{\mathrm{II}}(x,y) = z_*(x,y) + 2\delta(x,y)\cos\left(\theta_*(x,y) + \frac{4\pi}{3}\right) \in [0,1], \tag{A5b}$$

$$z^{\mathrm{III}} \equiv z^{\mathrm{III}}(x,y) = z_*(x,y) + 2\delta(x,y)\cos(\theta_*(x,y)) \ge 1 \tag{A5c}$$

with $z^{\mathrm{I}} < 0$ if and only if $\beta > 0$ and $z^{\mathrm{III}} > 1$ if and only if $\gamma > 0$. The zero z^{I} vanishes identically for $\beta = 0$, the zero z^{III} is identically equal to 1 for $\gamma = 0$.

Proof. Note first that A is always positive. One has in $\Re_+^2$

$$F(x,y,0) = +\beta x^2 \ge 0, \quad F(x,y,1) = -\gamma y^2 \le 0, \tag{A6}$$

$$\frac{d}{dz}F(x,y,0) = C(x,y) = x(\alpha - \beta x) \tag{A7a}$$

and

$$\frac{d}{dz}F(x,y,1) = 3A(x,y) + 2B(x,y) + C(x,y) = y(1 - 2\gamma y) \tag{A7b}$$

In case '$\beta > 0$, $\gamma > 0$' Eq. (A6) implies Eq. (A1) with strict inequalities. In case '$\beta = 0$, $\gamma > 0$' Eq. (A6) and $(d/dz)F(x,y,0) = \alpha x > 0$ (Eq. (A7a)) lead to Eq. (A1) with $z^{\mathrm{I}} = 0 < z^{\mathrm{II}} < 1 \le z^{\mathrm{III}}$. In case '$\beta > 0$, $\gamma > 0$' Eq. (A6) and $(d/dz)F(x,y,1) = y > 0$ (Eq. (A7b)) yield Eq. (A1) with $z^{\mathrm{I}} < 0 < z^{\mathrm{II}} < 1 = z^{\mathrm{III}}$. So we arrive in case '$\beta = 0$, $\gamma = 0$' at Eq. (A1) with $z^{\mathrm{I}} = 0 < z^{\mathrm{II}} < 1 = z^{\mathrm{III}}$.

These three simple zeros imply the existence of a strict local maximum (taken at $z = z_* - \delta$ and of a strict local minimum (taken at $z = z_* + \delta$) with values:

$$F(x,y,z_* - \delta(x,y)) = f_*(x,y) + h(x,y) > 0, \tag{A8a}$$

$$F(x,y,z_* + \delta(x,y)) = f_*(x,y) - h(x,y) < 0 \tag{A8b}$$

for $h(x,y) := 2A(x,y)\delta^3(x,y)$ implying $-1 \le -f_*(x,y)/h(x,y) \le +1$. Thereby, θ_* is well-defined by Eq. (A4) with:

$$\cos(\theta_*) \in \left[\frac{1}{2}, 1\right], \quad \cos\left(\theta_* + \frac{2\pi}{3}\right) \in \left[-1, -\frac{1}{2}\right] \quad \text{and}$$

$$\cos\left(\theta_* + \frac{4\pi}{3}\right) \in \left[-\frac{1}{2}, \frac{1}{2}\right]$$

Thus, Eqs. (A5a)–(A5c) follow from the substitution of $z = z_*(x,y) + 2\delta(x,y)\cos\theta$ into $F(x,y,z) = 0$ since

$$\begin{aligned} &F(x,y,z_*(x,y)) + 2\delta(x,y)\cos(\theta) \\ &\quad = h(x,y)[4\cos^3\theta - 3\cos\theta] + f_*(x,y) \\ &\quad = h(x,y)\cos(3\theta) + f_*(x,y) \overset{!}{=} 0 \end{aligned} \tag{A9}$$

can be rewritten as

$$\cos(3\theta) = -\frac{f_*(x,y)}{h(x,y)} \tag{A10}$$

References

[1] G. Guiochon, A. Felinger, D.S. Shirazi, A. Katti, Fundamentals of Preparative and Nonlinear Chromatography, Academic Press, New York, 2006.
[2] H. Schmidt-Traub, Preparative Chromatography of Fine Chemicals and Pharmaceutical Agents, WILEY-VCH Verlag, Weinheim, 2005.
[3] A. Seidel-Morgenstern, J. Chromatogr. A 1037 (2004) 255.
[4] A.L. Myers, J.M. Prausnitz, AIChE J. 11 (1965) 121.
[5] A.L. Myers, AIChE J. 29 (1983) 691.
[6] I. Langmuir, J. Am. Chem. Soc. 38 (1916) 2221.
[7] C.H. Giles, D. Smith, A. Huitson, J. Colloid Interface Sci. 47 (1974) 755.
[8] T.L. Hill, An Introduction to Statistical Thermodynamics, Addison-Welsley, Reading, 1960.
[9] G.A. Baker Jr., Graves-Morris, Padé Approximants, Cambridge University Press, Cambridge, 1996.
[10] D.M. Ruthven, Principles of Adsorption and Adsorption Processes, Wiley, New York, 1984.
[11] F. Gritti, G. Guiochon, J. Chromatogr. A 1028 (2004) 197.
[12] M. Moreau, P. Valentin, C. Vidal-Majdar, B.C. Lin, G. Guiochon, J. Colloid Interface Sci. 141 (1991) 127.
[13] D.B. Brougthon, Ind. Eng. Chem. 40 (1948) 1506.
[14] C.J. Radke, J.M. Prausnitz, AIChE J. 18 (1972) 761.
[15] A. Tarafder, M. Morbidelli, M. Mazzotti, 21st International Symposium on Preparative and Process Chromatography—PREP 2008, San Jose, USA, 15–18. 6. 2008, Poster P-223-T.
[16] R.W.D. Nickalls, Math. Gazette 77 (1993) 354.
[17] D. Redfern, C. Campbell, The Matlab 5 Handbook, Springer, New York, 1998.
[18] J.E.J. Dennis, in: D. Jacobs (Ed.), State of the Art in Numerical Analysis, Academic Press, New York, 1977.
[19] K. Levenberg, Quart. Appl. Math. 2 (1944) 164.
[20] D. Marquardt, Soc. Ind. Appl. Math., J. Appl. Math. 11 (1963) 431.
[21] J.J. Moré, in: G.A. Watson (Ed.), Numerical Analysis, Springer–Verlag, New York, 1977.
[22] F. Gritti, G. Guiochon, J. Chromatogr. A 1008 (2003) 23.
[23] A. Seidel-Morgenstern, G. Guiochon, Chem. Eng. Sci. 48 (1993) 2787.
[24] W. Zhang, Y. Shan, A. Seidel-Morgenstern, J. Chromatogr. A 1107 (2006) 216.
[25] P.V. Dankwerts, Chem. Eng. Sci. 2 (1953) 1.
[26] P. Rouchon, M. Schonauer, P. Valentin, G. Guiochon, Sep. Sci. Technol. 22 (1987) 1793.
[27] R. Courant, K. Friedrichs, H. Lewy, Math. Annalen 100 (1928) 32.